Comparison of high-resolution structures of the diphtheria toxin repressor in complex with cobalt and zinc at the cation-anion binding site

ARTICLE *in* PROTEIN SCIENCE · MAY 1997

Impact Factor: 2.85 · DOI: 10.1002/pro.5560060519 · Source: PubMed

5 AUTHORS, INCLUDING:

Randall K Holmes
University of Colorado
213 PUBLICATIONS **9,272** CITATIONS

SEE PROFILE

Protein Science (1997), *6*:1114–1118. Cambridge University Press. Printed in the USA.

FOR THE RECORD

Comparison of high-resolution structures of the diphtheria toxin repressor in complex with cobalt and zinc at the cation-anion binding site

EHMKE POHL,[1] XIAYANG QIU,[1,4] LISA M. MUST,[2] RANDALL K. HOLMES,[2] AND WIM G.J. HOL[1,3]

[1]Departments of Biological Structure and Biochemistry, The Biomolecular Structure Center, University of Washington, Box 357742, Seattle, Washington 98195-7742
[2]Department of Microbiology, University of Colorado, Health Sciences Center, Denver, Colorado 80262
[3]Howard Hughes Medical Institute, University of Washington, Box 357742, Seattle, Washington 98195-7742

(RECEIVED January 21, 1997; ACCEPTED March 10, 1997)

Abstract: The diphtheria toxin repressor (DtxR) from *Corynebacterium diphtheriae* is a divalent-metal activated repressor of chromosomal genes responsible for siderophore-mediated iron-uptake and of a gene on several corynebacteriophages that encodes diphtheria toxin. Even though DtxR is the best characterized iron-dependent repressor to date, numerous key properties of the protein still remain to be explained. One is the role of the cation-anion pair discovered in its first metal-binding site. A second is the reason why zinc exhibits its activating effect only at a concentration 100-fold higher than other divalent cations.

In the presently reported 1.85 Å resolution Co-DtxR structure at 100K, the sulfate anion in the cation-anion-binding site interacts with three side chains that are all conserved in the entire DtxR family, which points to a possible physiological role of the anion.

A comparison of the 1.85 Å Cobalt-DtxR structure at 100K and the 2.4 Å Zinc-DtxR structure at room temperature revealed no significant differences. Hence, the difference in efficiency of Co^{2+} and Zn^{2+} to activate DtxR remains a mystery and might be hidden in the properties of the intriguing second metal-binding site. Our studies do, however, provide a high resolution view of the cation-anion-binding site that has most likely evolved to interact not only with a cation but also with the anion in a very precise manner.

Keywords: *Corynebacterium diphtheriae*; diphtheria toxin repressor; metal-activated repressor; X-ray crystal structure

All pathogenic bacteria encounter iron-deficient growth conditions in vivo as most of the iron in the host is sequestered by iron- and heme-binding proteins. Many microorganisms have developed elaborate iron-uptake systems including siderophores and membrane-associated proteins in order to obtain iron from the host organism. Therefore, the regulation of iron uptake is a key factor in many pathogens (Weinberg, 1993; Mietzner & Morse, 1995). Here we report on an important iron-dependent regulator of the response of the bacteria to the iron concentration of the environment.

The diphtheria toxin repressor (DtxR) is an iron-activated protein that regulates expression of the diphtheria toxin gene that is carried by a family of corynebacteriophages (Barksdale 1970; Pappenheimer 1977). In *Corynebacterium diphtheriae*, DtxR also controls the expression of proteins of the iron-uptake system. In the presence of divalent iron, DtxR becomes activated as a repressor and binds as a homodimer to its target DNA-sequences, the *tox*, *irp1*, and *irp2* operators (Boyd et al. 1990; Tao et al., 1992, 1994; Schmitt & Holmes 1994). Whereas in vivo only Fe^{2+} acts as co-repressor, in vitro several other divalent transition metal ions including Fe^{2+}, Ni^{2+}, Co^{2+}, Mn^{2+}, and Cd^{2+} are activators. Quite remarkably, Zn^{2+} requires a concentration about two orders of magnitude greater than the other transition state metals in order to act as co-repressor (Tao & Murphy, 1992; Tao et al., 1994).

DtxR homologues have recently been discovered in several other pathogens, e.g., *Mycobacterium tuberculosis* (Schmitt et al., 1995), *M. leprae* (Doukhan et al., 1995), and nonpathogens, e.g. *Streptomyces pilosis*, *S. lividans* (Günther-Seeboth & Schupp, 1995), and in *Brevibacterium lactofermentum* (Oguiza et al., 1996), further emphasizing the importance of this class of proteins. Crystal structures of wild- type DtxR in complex with several different divalent transition metals have recently been solved and refined between 2.8 and 2.0 Å resolution (Qiu et al., 1995, 1996; Schiering et al., 1995). These structures revealed two metal-binding sites. One, designated metal-binding site 1, has been observed in all structures with high occupancy. The metal at this site is coordinated by Glu83, His98, His79, and, most intriguingly, also by one oxygen of a sulfate ion (Qiu et al., 1996). Hence, this metal-binding site is also called the "cation-anion"-binding site. Qiu et al. (1996) have also suggested that this anion near metal-binding

Reprint requests to: Wim G.J. Hol, Departments of Biological Structure and Biochemistry, The Biomolecular Structure Center, University of Washington, Box 357742, Seattle, Washington 98195-7742; e-mail hol@x-ray.bchem.washington.edu.

[4]Present address: Department of Macromolecular Sciences, Smith-Kline Beecham Pharmaceuticals, 709 Swedeland Road, King of Prussia, Pennsylvania 19406-0939

site 1 may function as a co-corepressor. The second transition metal-binding site in wild-type DtxR has so far only been observed in the Cd-DtxR (Qiu et al., 1995) and Mn-DtxR structures (Qiu et al., 1996). In the crystal structure of the Cys102Asp DtxR variant, determined by Ding et al. (1996), a nickel-binding site is described near site 2 in the wild-type structure. The present paper focuses on the comparison of the zinc- and cobalt-containing repressors.

Results and discussion

Our present models for Co-DtxR and Zn-DtxR consist of amino acid residues 4–140, 148–198, 201–223, one metal ion, and one anion. In addition, the Co-DtxR model contains residues 224–226 and 175 solvent molecules, and the Zn-DtxR structure 72 solvent molecules, respectively. The structures are refined to R-values of 21.8% (Co-DtxR) and 18.2% (Zn-DtxR) with good geometry (Table 1). All residues are in allowed regions of the Ramachandran diagram. The first two domains have well defined density. However, even at 1.85 Å resolution, at 100 K, the third domain (residues 148–226) in Co-DtxR appears to be partially disordered.

In the 1.85 Å cobalt-sulfate-DtxR structure at 100 K, the metal at site 1 is coordinated tetrahedrally by $N^{\delta 1}$ of His79, $O^{\epsilon 1}$ of Glu83, $N^{\epsilon 2}$ of His98, and a sulfate anion oxygen (Fig. 1A, Table 2). The inital F_o-F_c difference (Fig. 2A) electron density, calculated before the sulfate or any solvent molecules were included in the refinement, shows very clearly a tetrahedrally-shaped density for the sulfate anion that makes hydrogen bonds to the $N^{\eta 1}$ and N^{ϵ} of Arg80, $N^{\delta 2}$ of Asn130, O^{γ} of Ser126, and to the solvent molecules 301, 336, and 351. It is of great potential functional significance that each oxygen atom of the sulfate is liganded by at least one protein side chain atom. It is noteworthy that Arg80, Ser126, and Asn130 are completely conserved among all known members of the DtxR family (Doukhan et al., 1995; Günther-Seeboth & Schupp, 1995; Schmitt et al., 1995; Oguiza et al., 1996). The evolutionarily conserved exquisite coordination of the anion by the protein suggests a functional role, possibly being on the communication pathway between metal-binding site 1 and DNA-binding helix 2 in the first domain.

Table 1. *Crystallographic data and refinement statistics*

	Co-DtxR	Zn-DtxR
Crystal dimensions [mm]	0.5 × 0.3 × 0.2	0.3 × 0.3 × 0.2
Temperature [K]	100	293
Space group	$P3_121$	$P3_121$
Cell dimensions [Å]	a = 63.6	a = 64.3
	b = c = 107.2	b = c = 109.3
No. of refl. collected	120,923	74,318
Resolution [Å]	1.85	2.40
Completeness [%]	99.6	98.6
R-merge (on intensities)	0.050	0.091
No. of refl. used	21682	10217
No. protein atoms	1659	1589
No. of solvent atoms	175	72
R-factor	21.8	18.2
R-free	28.7	26.7
R.m.s. deviation from ideality:		
Bond distances [Å]	0.012	0.011
Bond angles (degrees)	1.7	1.7

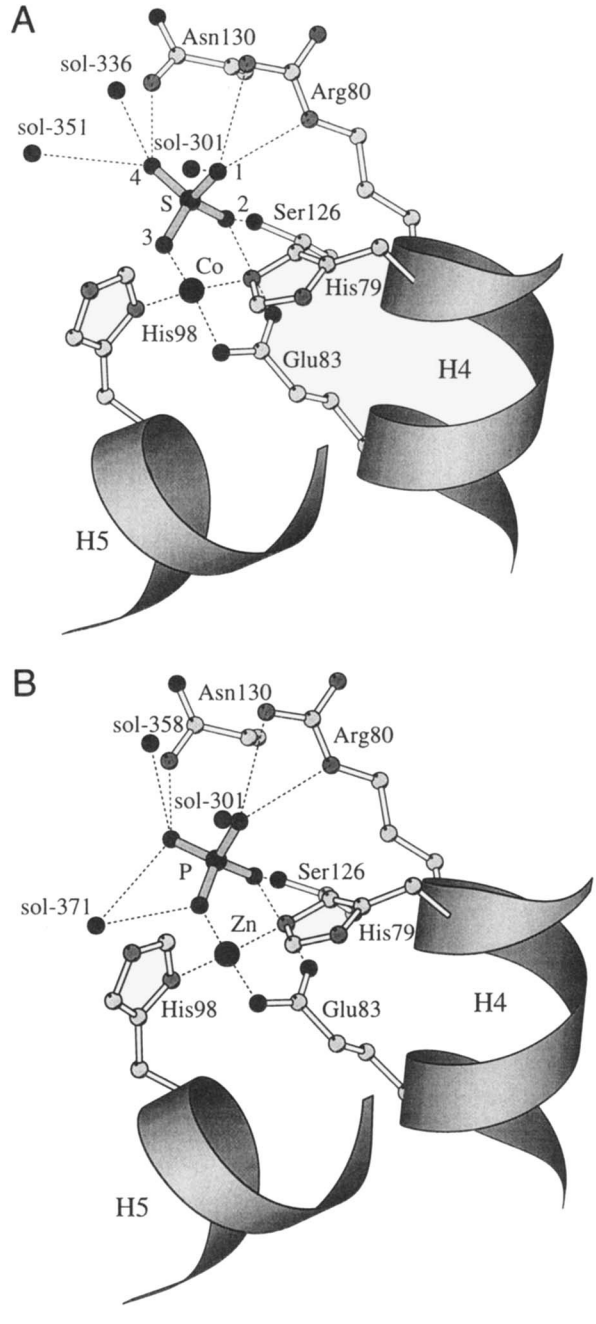

Fig. 1. Close-up of the cation-anion-binding site in DtxR. Hydrogen bonds are depicted as dashed lines. **A:** 1.85 Å cobalt-DtxR at 100K. **B:** 2.4 Å Zinc-DtxR at 293K. The geometry of the binding sites in the 1.85 Å Co and 2.4 Å Zn DtxR-structures are very similar (Table 2)—the only apparent differences are the solvent ions. All figures were prepared using MOLSCRIPT (Kraulis, 1991) and O (Jones et al., 1991).

The second metal-binding site in wild-type Cd-DtxR and Mn-DtxR (Qiu et al., 1995, 1996) is ~10 Å removed from metal-binding site 1. In these structures, the ligands of site 2 are the carbonyl oxygen of Cys102, the $O^{\epsilon 1}$ of Glu105, the $N^{\epsilon 2}$ of His106, and a solvent (probably a water) molecule. In our new 1.85 Å Co-DtxR structure at 100K, site 2 is not occupied by a metal ion. The closest difference peak at 5.5 sigma lies 1.3 Å from this site with reasonable distances for a solvent molecule and therefore was

Table 2. *Geometry of the metal binding site 1 in Co-DtxR and Zn-DtxR*

	Co-DtxR	Zn-DtxR
Distance [Å]:		
Me-$N^{\epsilon 2}$ His79	2.0	2.1
Me-$O^{\epsilon 1}$ Glu83	2.0	1.9
Me-$N^{\delta 1}$ His98	2.0	1.9
Me-O3 SO_4/PO_4	2.0	1.9
Angles (degrees):		
$O^{\epsilon 1}$-Me-$N^{\epsilon 2}$	96	106
$N^{\delta 1}$-Me-$O^{\epsilon 1}$	114	114
O3-Me-$N^{\delta 1}$	106	106
$O^{\epsilon 1}$-ME-O3	109	103
$N^{\epsilon 2}$-Me-O3	122	112
$N^{\delta 1}$-Me-$N^{\epsilon 2}$	111	115
Sulfate/phosphate site (distances in Å):		
O1-$N^{\epsilon 1}$ Arg80	3.0	3.2
O1-$N^{\zeta 2}$ Arg80	3.0	3.1
O1-solvent	2.7	2.8
O2-O^{γ} Ser126	2.6	2.8
O2-$O^{\epsilon 2}$ Glu83	2.8	2.9
O3-solvent371	absent	2.8
O4-$N^{\delta 2}$ Asn130	2.6	2.7
O4-solvent336/358[a]	2.9	3.2
O4-solvent351/371[b]	3.3	3.3

[a]This is solvent number 336 in the Co-DtxR structure and solvent 358 in the Zn-DtxR structure.

[b]This is solvent number 351 in Co-DtxR and solvent 371 in Zn-DtxR

refined as a water molecule. The reason for the lack of metal-binding at site 2 is probably a chemical modification of the sulfur atom of Cys102 as described by Qiu et al. (1995, 1996). In the 1.85 Å Co-DtxR (F_o-F_c) difference electron density, after including the occupants of the cation-anion-binding site in the model, the highest maximum of 13 sigma occurs at a position approximately 2 Å from the S^{γ} of Cys102 with a "C^{β}-S^{γ}-X" angle of 95 degrees. There is additional electron density visible beyond this maximum which was not visible in the 2.0 Å room-temperature Co-DtxR structure (Fig. 3). However, it was not possible, even by mass spectrometry, to identify the chemical nature of this modification.

The Zn^{2+}-DtxR crystal was obtained with a high citrate concentration as precipitant and there was no sulfate present during preparation and crystallization. Yet, after including a Zn ion at site 1, in the first difference electron density the highest maximum of 13 sigma was exactly at the sulfate position associated with metal-binding site 1 in the other DtxR structures grown from sulfate and selenate (Qiu et al., 1995, 1996). Furthermore, the shape of the density and the distance of the maximum to the metal ion suggested the presence of something heavier and larger than just a water molecule and more compact than a citrate anion (Fig. 2B). We suggest that in this Zn-DtxR structure the position might be filled with a phosphate anion because 10 mM phosphate buffers were used during the preparation of the protein (Schmitt & Holmes, 1993). Refinement of this peak at the anion-binding site as a phosphate with full occupancy resulted in a relatively low B-factor of 38 $Å^2$ for the phosphorous atom and an average B-factor of 41 $Å^2$ for the oxygen atoms.

The highest maximum near binding site 2 in the zinc-containing repressor was only a 3.2 sigma peak with reasonable distances for a solvent molecule. Hence, it appears that site 2 is empty in Zn-DtxR, except for a water molecule—presumably for the same reason as discussed above for Co-DtxR. As in the 1.85 Å Cobalt-DtxR structure, after including the phosphate in the refinement of Zn-DtxR, the strongest peak in the difference electron density appeared at a position close to S^{γ} of Cys102. The maximum peak height was 9 sigma. However, at this lower resolution no significant electron density is visible beyond the supposed "Sδ-atom" at Cys102.

The overall structures of Co-DtxR, at 1.85 Å resolution and 100 K, and of Zn-DtxR at 2.4 Å and 293 K, are essentially the same. The r.m.s. deviation of 136 alpha-carbon atoms of the first two domains of these two structures is only 0.4 Å. The superposition of all non-hydrogen atoms of residues 79, 83, and 98 forming the metal-binding site resulted in an r.m.s. deviation of only 0.2 Å. The Co and Zn positions at site 1 differ by only 0.2 Å in the two structures, whereas the centers of the anions differ by only 0.1 Å. Clearly, the cobalt and zinc DtxR structures are very similar overall as well as with regard to the precise details of the cation-anion-binding site (see also Table 2). Although our present studies have not explained the finding that zinc is required at a 100-fold higher concentration than other divalent cations to activate DtxR (Tao & Murphy, 1992), they provide structural information about the cation-anion-binding site at high resolution and strengthen the hypothesis that both the cation and anion at this site are important for the structure and function of DtxR.

Materials and methods

DtxR was overexpressed in *E. coli* and purified using a Ni-NTA affinity column followed by anion exchange chromatography as described earlier (Schmitt et al. 1992; Schmitt & Holmes 1993). DtxR in complex with cobalt and sulfate was crystallized in hanging drops. A volume of 4 μL of a protein solution in 10 mM TRIS buffer, pH 8, 50mM NaCl, and 5 mM DTT was mixed with 2 μL of a well solution containing 1.8 M ammonium sulfate, 100 mM TRIS pH 8.5, 10 mM $CoCl_2$ (Qiu et al., 1995). Before data collection, the crystal was transferred in a cryoprotectant consisting of 20% glycerol, 1.2 M ammonium sulfate, 67 mM TRIS pH 8.5, and 6.7 mM $CoCl_2$. The crystal was transferred into a rayon loop and flash-frozen in the cold nitrogen stream (Teng, 1990). Data were collected at beam line 7-I at the SSRL synchrotron, Stanford, using a MAR image plate as detector. The wavelength was 1.008 Å.

Crystals of DtxR complexed with zinc and phosphate were obtained over a period of nine months from a sitting drop containing equimolar amounts of DtxR and an oligonucleotide in 10 mM TRIS buffer pH 7.2 equilibrated against 50% saturated sodium citrate solution in 50 mM HEPES buffer pH 7.5, 5 mM 2-mercaptoethanol, and 10 mM $ZnCl_2$. The crystal was mounted in a capillary. Data were collected at room temperature on an RAXIS-II using monochromatic CuK^{α} radiation and focusing mirrors. In both cases, the data were integrated and scaled using DENZO and SCALEPACK (Otwinowski, 1992). Crystallographic refinement was performed with XPLOR (Brünger et al., 1987) using the coordinates of the protein of the Co-DtxR structure at 2.0 Å as the starting point. The solvent atoms and the sulfate/phosphate coordinates were not used to calculate the initial F_o-F_c electron density maps. Five percent of the data were used to calculate the free R-values (Brünger, 1993). The crystallographic data are summarized in Table 1. In order to avoid any bias from the force field all charges of the metal, the atoms of the sulfate/phosphate and the

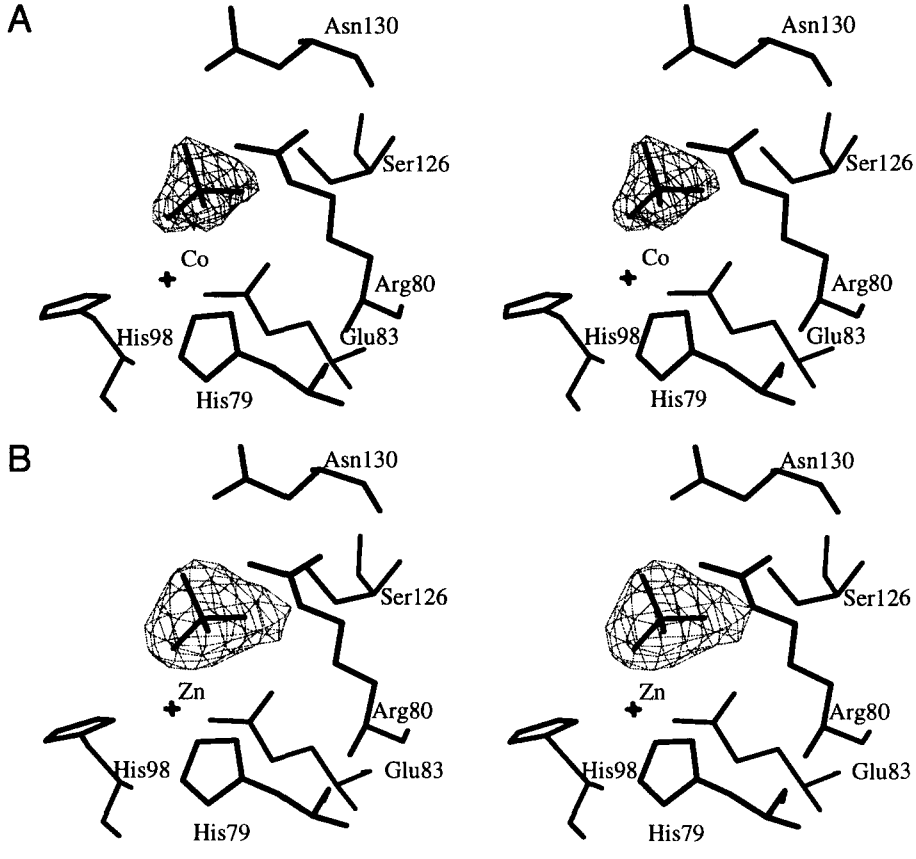

Fig. 2. Initial F_o-F_c electron density omit map at 3.0 sigma level showing the position of the sulfate at metal binding site 1 for (a) Co-DtxR and (b) Zn-DtxR crystal grown in absence of sulfate. The density for the postulated phosphate site in Zn-DtxR is clearly tetrahedral. The anion density in Zn-DtxR at 2.4 Å is also very similar in shape and size as the 2.2 Å structure of Mn-DtxR (Qiu et al., 1996, not shown).

ligating residues were set to zero. The ligating histidines (residues 79 and 98) were refined without any hydrogens to avoid the repulsive Van der Waals terms. All model building and inspection of electron density maps were done using O (Jones et al., 1991).

Acknowledgments: This work was supported by the NIH grant R01CA65656 to W.G.J.H. and NIH grant R01AI14107 to R.K.H., and by a major equipment grant from the Murdock Charitable Trust to the Biomolecular Structure Center. We thank the SSRL staff and Steven Suresh for their help during data collection, our colleagues at the Biomolecular Structure Center for stimulating discussion, Christophe Verlinde and Ethan Merritt for installing and maintaining computer systems, and Stewart Turley for maintaining the area detectors. E.P. is grateful to the Schering Research Foundation for a postdoctoral fellowship.

References

Barksdale L. 1970. *Corynebacterium diphtheriae* and its relatives. *Bacteriol Rev* *34*:378–422.

Boyd J, Oza MN, Murphy JR. 1990. Molecular cloning and DNA sequence

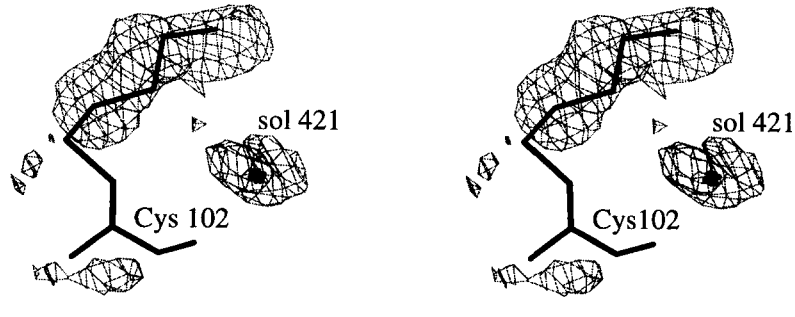

Fig. 3. F_o-F_c electron density map of Co-DtxR showing the additional density at Cys102. The final model included S^{δ}, C^{ϵ}, C^{ζ}, and C^{ξ} as hypothetical atoms to represent this density in an approximate way. The map shown was calculated before adding these atoms to the model.

analysis of a diphtheria-*tox* iron-dependent regulatory element (dtxR) from *Corynebacterium diphtheriae*. *Proc Natl Acad Sci USA 87*:5968–5972.

Brünger AT. 1993. Assessment of phase accuracy by cross validation: The free R value, methods and applications. *Acta Cryst D49*:24–36.

Brünger AT, Kuriyan J, Karplus M. 1987. Crystallographic R-factor refinement by molecular dynamics. *Science 235*:458–460.

Ding X, Zeng H, Schiering N, Ringe D, Murphy JR. 1996. Identification of the primary metal ion-activation sites of the diphtheria *tox* repressor by X-ray crystallography and site-directed mutational analysis. *Nat Struct Biol 3*:382–387.

Doukhan L, Predich M, Nair G, Dussurget O, Mandic-Mulec I, Cole ST, Smith DR, Smith I. 1995. Genomic organization of the mycobacterial sigma gene cluster. *Gene 165*:67–70

Günther-Seeboth K, Schupp T. 1995. Cloning and sequence analysis of the *Corynebacterium diphtheriae* dtxR homologue from *Streptomyces lividans* and *S. pilosus* encoding a putative iron repressor protein. *Gene 166*:117–119.

Jones TA, Zou JY, Cowan SW, Kjeldgaard M. 1991. Improved methods for building protein models in electron density maps and the location of errors in these models. *Acta Crystallogr A47*:110–119.

Kraulis P. 1991. MOLSCRIPT: A program to produce both detailed and schematic plots of protein structures. *J Appl Cryst 24*:946–950.

Mietzner TA, Morse SA. 1995. The role of iron-binding proteins in the survival of pathogenic bacteria. *Annu Rev Nutr 14*:471–493.

Oguiza JA, Marcos AT, Malumbres M, Martin JF, 1996. Multiple sigma factor genes in *Brevibacterium lactofermentum*: Characterization of *Sig A* and *Sig B*. *J Bacteriol 178*:550–553.

Otwinowski Z. 1993. Oscillation data reduction program. In: Swayer L, Isaacs N, Gailey S, eds. *Proceeding of the CCP4 Study Weekend, data collection and processing, 29–30 January*. England: SERC Daresbury Laboratory. pp 56–62.

Pappenheimer AM. 1977. Diphtheria toxin. *Annu Rev Biochem 46*:69–94.

Qiu X, Pohl E, Holmes RK, Hol WGJ. 1996. High-resolution structure of the diphtheria toxin repressor complexed with cobalt and manganese reveals an SH3-like third domain and suggests a possible role of phosphate as co-corepressor. *Biochemistry 35*:12292–12302.

Qiu X, Verlinde CLMJ, Zhang S, Schmitt MP, Holmes RK, Hol WGJ. 1995. Three-dimensional structure of the diphtheria toxin repressor in complex with divalent cation co-repressors. *Structure 3*:87–100.

Schiering N, Tao X, Zeng H, Murphy JR, Petsko GA, Ringe D. 1995. Structures of the apo- and metal ion-activated forms of the diphtheria toxin repressor from *Corynebacterium diphtheriae*. *Proc Natl Acad Sci USA 92*:9843–9850.

Schmitt MP, Holmes RK. 1993. Analysis of diphtheria toxin repressor-operator interactions and characterization of a mutant with decreased binding activity for divalent metals. *Mol Microbiol 9*:173–181.

Schmitt MP, Holmes RK. 1994. Cloning, sequence, and footprint analysis of two promotor/operators from *Corynebacterium diphtheriae* that are regulated by the diphtheria toxin repressor (DtxR) and iron. *J Bacteriol 176*:1141–1149.

Schmitt MP, Predich M, Doukhan L, Smith I, Holmes RK. 1995. Characterization of an iron-dependent regulatory protein (IdeR) of *Mycobacterium tuberculosis* as a functional homolog of the diphtheria toxin repressor (DtxR) from *Corynebacterium diphtheriae*. *Infect Immun 63*:4284–4289.

Schmitt MP, Twiddy EM, Holmes RK. 1992. Purification and characterization of the diphtheria toxin repressor. *Proc Natl Acad Sci USA 89*:7576–7580.

Tao X, Boyd J, Murphy JR. 1992. Specific binding of the diphtheria *tox* regulatory element DtxR to the *tox* operator requires divalent heavy metal ions and a 9 base-pair interrupted palindromic sequence. *Proc Natl Acad Sci USA 89*:5897–5901.

Tao X, Murphy JR. 1992. Binding of the metalloregulatory protein DtxR to the diphtheria *tox* operator requires a divalent heavy metal ion and protects the palindromic sequence from DNase I digestion. *J Biol Chem 30*:21761–21764.

Tao X, Schiering N, Zeng H, Ringe D, Murphy JR. 1994. Iron, DtxR, and the regulation of diphtheria toxin expression. *Mol Microbiol 14*:191–197.

Teng TY. 1990. Mounting of crystals for macromolecular crystallography in a free-standing thin film. *J Appl Crystallogr 23*:387–391.

Weinberg ED. 1993. The development of awareness of iron-withholding defense. *Prospect Biol Med 36*:215–221.